J Mater Sci: Mater Med (2010) 21:1255–1262
DOI 10.1007/s10856-009-3878-y

Biocompatibility of individually designed scaffolds with human periosteum for use in tissue engineering

Stephan T. Becker · Timothy Douglas · Yahya Acil · Hermann Seitz · Sureshan Sivananthan · Jörg Wiltfang · Patrick H. Warnke

Received: 27 May 2009 / Accepted: 17 September 2009 / Published online: 7 February 2010
© Springer Science+Business Media, LLC 2010

Abstract The aim of this study was to evaluate and compare the biocompatibility of computer-assisted designed (CAD) synthetic hydroxyapatite (HA) and tricalciumphosphate (TCP) blocks and natural bovine hydroxyapatite blocks for augmentations and endocultivation by supporting and promoting the proliferation of human periosteal cells. Human periosteum cells were cultured using an osteogenic medium consisting of Dulbecco's modified Eagle medium supplemented with fetal calf serum, Penicillin, Streptomycin and ascorbic acid at 37°C with 5% CO_2. Three scaffolds were tested: 3D-printed HA, 3D-printed TCP and bovine HA. Cell vitality was assessed by Fluorescein Diacetate (FDA) and Propidium Iodide (PI) staining, biocompatibility with LDH, MTT, WST and BrdU tests, and scanning electron microscopy. Data were analyzed with ANOVAs. Results: After 24 h all samples showed viable periosteal cells, mixed with some dead cells for the bovine HA group and very few dead cells for the printed HA and TCP groups. The biocompatibility tests revealed that proliferation on all scaffolds after treatment with eluate was sometimes even higher than controls. Scanning electron microscopy showed that periosteal cells formed layers covering the surfaces of all scaffolds 7 days after seeding. Conclusion: It can be concluded from our data that the tested materials are biocompatible for periosteal cells and thus can be used as scaffolds to augment bone using tissue engineering methods.

S. T. Becker (✉) · T. Douglas · Y. Acil · J. Wiltfang · P. H. Warnke
Department of Oral and Maxillofacial Surgery, Christian-Albrechts-University of Kiel, Arnold-Heller-Str. 3, Haus 26, 24105 Kiel, Germany
e-mail: becker@mkg.uni-kiel.de; Mail@st-becker.de

H. Seitz
Fluid Technology and Microfluidics, University of Rostock, Rostock, Germany

S. Sivananthan
Epsom and St. Helier University Hospitals NHS Trust and South West London Elective Orthopaedic Centre, University College London, London, UK

P. H. Warnke
Faculty of Health Sciences and Medicine, Bond University, Gold Coast, QLD, Australia

1 Introduction

The cultivation of large bone replacements to treat defects due to congenital malformations, trauma, infection or tumor resection remains a challenge today. Although significant advances in development of bone substitutes—also for smaller augmentations—have been made in the last decades, transplantation of autologous bone grafts is still the preferred therapy [1, 2]. Nevertheless autografts increase morbidity at the donor site and are limited in size and availability [1].

In vivo tissue engineering techniques such as intramuscular endocultivation, where the patient serves as his own bioreactor, have yielded customized and vascularized bone grafts that have been used to reconstruct the patient's skeleton [3, 4]. But homogeneous ossification inside the graft and form consistency of the endocultivated bone is still not completely predictable.

Biomaterials play a central role in tissue engineering approaches, presenting biophysical and biochemical milieus that direct cellular behavior and function [2]. Hydroxyapatite (HA) and Tricalciumphosphate (TCP) are widely used in orthopedic and maxillofacial applications

[2, 5–8]. Combinations of HA and TCP are also used [9] in addition to other materials [10].

Larger and individually designed scaffolds often consist of several material combinations, e.g. titanium to guarantee form consistency and hydroxyapatite for bone formation. The rapid prototyping technique of 3D printing allows for manufacture of complex-shaped porous ceramic matrices directly from computer data. Anatomical information obtained from a patient can be used to design a custom-made implant for a target defect [4, 11]. Besides shape, this process also allows different pore sizes or rounded surface patterns to be designed.

All these engineered bone grafts have no periosteal layer at the beginning. Without a periosteum the instant or rapid development of a substantial cortical layer is unlikely [12] especially with long bones. A promotion of cortical bone growth may increase stability of dental implants in clinical practice.

However, little is known about biocompatibility of scaffold materials used for tissue engineering materials towards periosteum even though they are in the vicinity of each other [13]. The osteoinductive and nutritious capabilities of the periosteum are well known [14–16]. Periosteal cells proliferate faster than marrow stromal cells [17]. It is remarkable that periosteum contains many osteoprogenitor cells that show high bone formation rates in animal models [18]. It is also a source for mesenchymal stem cells [19]. Thus, periosteal cells may have important advantages for bone tissue engineering [20] and oral implantology, as they are able to induce bone formation and may induce a cortical margin and reduce bone overgrowth outside the scaffolds.

Periosteum can be harvested easily during oral surgery. Periosteal cell cultivation and proliferation to enhance cell numbers can be performed in vitro [21]. In an earlier study, we found collagen membranes were well suited for the cultivation of periosteum layers [13].

The aim of this study was to test the three scaffolds of 3D-printed hydroxyapatite, 3D-printed tricalciumphosphate and bovine hydroxyapatite for their biocompatibility and ability to support and promote the proliferation of human periosteal cells.

2 Materials and methods

2.1 Isolation and cultivation of cells from periosteum

Human periosteum biopsies were harvested from patients during the course of oral surgery (wisdom tooth removal). The study was approved by the ethics board of the University of Kiel (A 417/07). The cells were cultivated using an osteogenic medium consisting of Dulbecco's modified Eagle medium (DMEM) supplemented with 10% fetal calf serum (FCS), 100 IE Penicillin/ml, 100 µg Streptomycin/ml and 1 mmol/l ascorbic acid at 37°C with 5% CO_2. Cell seeding was performed after the second passage. During passaging, cells were detached from 75 cm^2 cell culture flasks using 5 ml of a 0.05% trypsin/0.02% EDTA solution in Phosphate Buffered Saline (PBS). After 1:1 dilution of the cell suspension with DMEM containing 10% FCS and centrifugation at $3200 \times g$ for 3 min, cells were resuspended in DMEM containing 10% FCS, counted and reseeded at a density of 10^5 cells per 75 cm^2 cell culture flask. Cells were cultured in the same medium used for cell seeding in a humidified atmosphere with 5% CO_2 at 37°C. Medium change took place every 3 days.

2.2 Matrices

The following three matrices served as scaffolds for cultivation of the cells: 3D-printed hydroxyapatite, 3D-printed TCP and bovine hydroxyapatite (BioOss, Geistlich AG Wolhusen, CH).

The 3D printing process is a powder-based process that builds physical 3D models layer-by-layer directly from computer data [22, 23]. The process started with a three-dimensional dataset that was sliced by a computer into a stack of two-dimensional bitmap-files. The bitmap-files represented the print matrices of the corresponding cross-sections of the part to be built. The 3D printer laid out a thin layer of granulates onto the top of the building box. Liquid binder was printed on the layer of powder according to the current print matrix using a micro-dispensing valve. The ceramic powder was bonded in these selected regions. When the layer was completed, the building box piston moved down by the thickness of a layer and a new layer of powder was deposited on the first one. These process steps were repeated until the whole part was built within the powder bed. The part was surrounded and supported by loose, unbound powder. After completion, the part was removed from the building box and cleaned using an air blower. Finally, the 3D-printed ceramic green bodies were consolidated at a temperature of 1250°C. Two spray-dried granulates HA19 and TCP4 were obtained from BioCer Entwicklungs-GmbH (Bayreuth, Germany) and used as raw materials for 3D printing of HA and TCP scaffolds. The mean diameter of the granulates was well below 100 µm. HA granules had a mean diameter d_{50} of 32 µm and TCP granules had a larger mean diameter d_{50} of 52 µm. The processing of these materials by 3D printing has been investigated in a previous study [24]. An aqueous solution of dextrin (20 wt%) and saccharose (2.5 wt%) was used as printing binder. The printing raster resolution and the thickness of the powder layers were chosen as 0.25 mm for all specimens. The 3D printed specimens were sintered

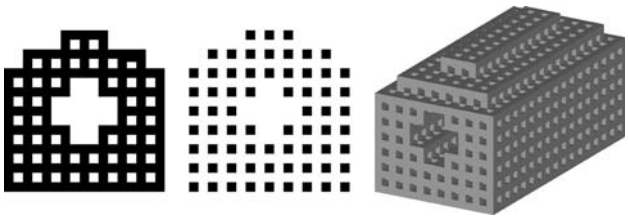

Fig. 1 Exemplary illustration of two different bitmaps that are used as printing matrices (*left*, *middle*). 3D rendering of the specimen with regular quadratic channel structure (*right*)

for 2 h at 1250°C in a high temperature furnace (Nabertherm, Germany) in ambient air. The organic binder was burnt out and the 3D printed part obtained its final properties during sintering. The sintering typically causes shrinkage of the ceramic green body. This sintering shrinkage is highly reproducible. Therefore, the shrinkage effect can be compensated for by scaling the CAD model prior to printing.

In this study, the specimen was designed by directly generating the stack of bitmaps for the 3D printer. The stack of bitmaps was created by drawing and copying several bitmaps using Corel Paint Shop Pro (Corel Corporation, Canada). Two exemplary bitmaps as well as a 3D rendering of the specimen are depicted in Fig. 1. The external dimensions of the specimen were $12.75 \times 12.75 \times 24.75$ mm^2. The bar width and a bar distance of the internal pore network was 0.75 mm in both cases. Since shrinkage took place during sintering all dimensions of the final specimens were smaller.

The scaffolds were divided into quadratic pieces of side length 7 mm and placed in 24-well cell culture plates (Nunc, Germany). Cells were seeded on scaffold pieces at a density of 10^4 cells/well. Cells were cultured on scaffold pieces in 2000 µl of the same medium used for cell seeding in a humidified atmosphere with 5% CO_2 at 37°C. Medium change took place every 3 days. At these points cultures were checked microscopically.

2.3 Assessment of cell vitality

Cell vitality was assessed by Fluorescein Diacetate (FDA) and Propidium Iodide (PI) staining. Staining was performed on cells cultured in eluate from scaffolds after 24 h incubation in cell culture medium. 5×10^3 cells in cell culture medium with 10% FCS were seeded on 8-well objectives. After 1 day of culture, 200 µl eluate from scaffolds immersed in serum-free cell culture medium for 24 h was added to cells. After 24 h incubation at 37°C and 5% CO_2, cells were rinsed with PBS and immersed in an FDA solution made by diluting 30 µl × 1 mg FDA/ml acetone in 10 ml PBS. After incubation for 15 min at 37°C in the dark, the FDA solution was removed by suction and replaced with a PI solution made by diluting 500 µl × 1 mg/ml PI in 10 ml PBS. After incubation for 2 min at room temperature in the dark, scaffolds were rinsed twice in PBS. While still immersed in PBS, scaffolds were then subjected to fluorescence microscopy with excitation at 488 nm and detection at 530 nm (FDA, green) and 620 nm (PI, red).

2.4 Biocompatibility tests

Tests were performed according to the protocols of another study [13].

2.5 LDH and BrdU, MTT and WST tests

LDH tests can show cell death and lysis. Cells were seeded in 96-well cell culture plates (Nunc, Germany) in 100 µl DMEM at a concentration of 5×10^3 cells/well. After 24 h culture in a humidified atmosphere with 5% CO_2 at 37°C, medium was removed and replaced with 150 µl eluate from the scaffolds. Cells cultured in 2% Triton-X-100 in serum-free DMEM served as high controls. Cells cultured in serum-free DMEM served as low controls. After 24 h incubation, 100 µl eluate was transferred to another 96-well cell culture plate. Extracellular LDH activity was measured with the help of an LDH Detection Kit (Roche Diagnostics, Mannheim, Germany, Cat. No. 11644793001). Absorbance was measured at 490 nm. The remaining 50 µl eluate per well remaining in the cell culture plate was removed and replaced with 100 µl DMEM containing 10% fetal calf serum (FCS), Penicillin/ml, 100 µg Streptomycin/ml and 1 mmol/l ascorbic acid. After 7 days incubation, proliferation was measured with the help of a BrdU Cell Proliferation ELISA Kit (Roche Diagnostics, Mannheim, Germany, Cat. No. 11647229001). Absorbance was measured at 450 nm.

After 24 h incubation with eluate from the scaffolds, proliferation was assessed with the aid of a MTT Cell Proliferation Kit (Roche Diagnostics, Mannheim, Germany, Cat. No. 11465007001). Calibration curves of $0.16–10 \times 10^3$ cells/well served as standards. Absorbance was measured at 450 nm.

As mentioned previously, scaffold pieces were seeded at a density of 10^4 cells/piece. After 7 days culture in 2000 µl cell culture medium, proliferation was assessed with the aid of a Cell Proliferation Reagent WST-1 (Roche Diagnostics, Mannheim, Germany, Cat. No. 116446807001). Briefly, 200 µl WST-1 reagent was added to each well at a 1:10 ratio to cell culture medium. After 4 h incubation in a humidified atmosphere with 5% CO_2 at 37°C, medium was transferred to 96-well plates and absorbance was measured at 450 nm. Cells cultured in wells without scaffold pieces at a density of 10^4 cells/well served as controls.

2.6 Scanning electron microscopy (SEM) examinations

Scanning electron microscopy (SEM) investigations were carried out 1 week after cell seeding using a XL30CP device (Phillips Electron Optics GmbH, Kassel, Germany) operating at 10–25 kV, as used by Yang et al. [25]. As preparation for the SEM investigation, cell-seeded scaffolds and scaffolds without cells as controls were first rinsed using phosphate buffered saline (PBS) to remove cell culture medium. Cells were then fixed using 3% glutaraldehyde in PBS at pH 7.4 for 24 h. After removal of glutaraldehyde solution, cells were dehydrated by incubating scaffolds in a series of ethanol solutions of increasing concentration. Scaffolds were immersed for 5 min in each of the following ethanol dilutions: 50, 60, 70, 80, 90 and 100%. Subsequently critical point drying was performed using a K850 Critical Point Dryer (Emitech, USA) followed by gold sputtering with an SCD 500 device (CAL-Tec, Ashford, UK).

2.7 Statistical evaluation

Absorbance values of the tests were related to the mean results obtained without scaffold materials. All values of the LDH test were divided by 0.33 (mean of low control), the values of the MTT test by 0.46, the WST results by 0.77 and the BrdU values by 1.18. These results were analysed by ANOVAS for each test with the factors *material* (printed HA, printed TCP and bovine HA) and *time* (10 min, 1 and 24 h). Least squared means and 95% confidence intervals are presented in text and figures.

3 Results

3.1 Assessment of cell vitality on scaffolds

After 24 h all probes showed viable periosteal cells. The green color of the cells due to Fluorescein Diacetate (FDA) staining demonstrated their vitality on all scaffolds, while there were red cells visible despite Propidium Iodide (PI) staining indicating some dead cells for the bovine HA group, while only very few red cells were visible for the printed HA and printed TCP and no red cells in the control group. These results are illustrated in Fig. 2.

3.2 Biocompatibility tests

In the case of the LDH test, cytotoxicity of all scaffolds after treatment with eluate was lower than the low control

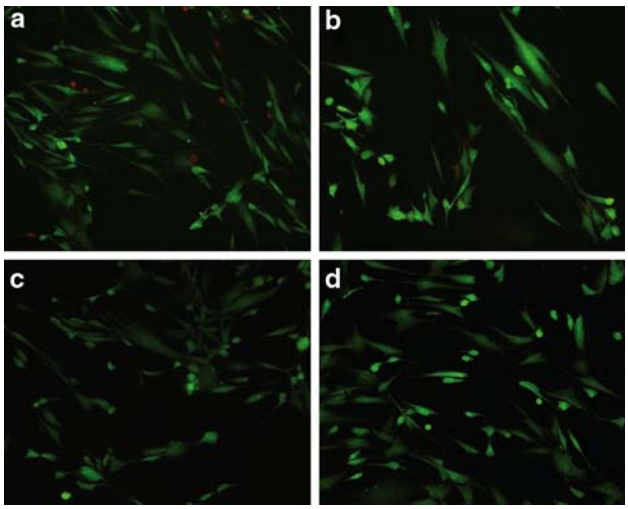

Fig. 2 Fluorescence microscopy images of human periosteal cells after staining with Fluorescein Diacetate (green) and Propidium Iodide (red = dead cells): Note the green color indicating living cells. Some dead cells appeared for the bovine HA group, while only very few red cells were visible for the printed HA and printed TCP and no red cells in the control group. **a** Bovine HA; **b** printed HA; **c** printed TCP; **d** control

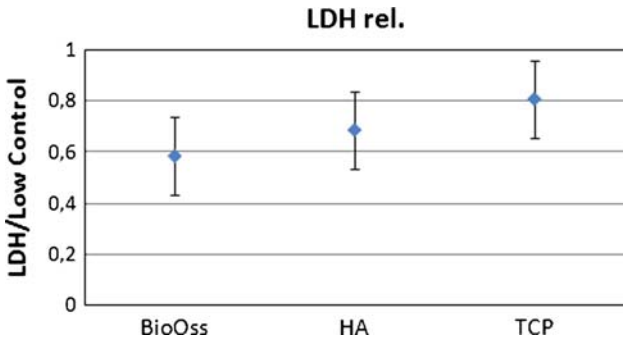

Fig. 3 LDH test of cells from human periosteum on bovine HA, printed HA and printed TCP. Values are lower than the low control for all materials

(zero cytotoxicity; see Fig. 3). There was no statistically significant difference between the materials ($P = 0.126$).

The MTT test gives a measure of cellular metabolic activity dependent on living cells, proliferation, viability and cytotoxicity. At a later point than MTT, the WST test indicates the metabolic activity of cells. In the case of the MTT test, metabolic activity was higher than the control (>1) for the scaffolds and the materials showed different results ($P < 0.0001$; see Fig. 4). The WST test revealed values around 0.6 for the printed HA and 0.9 for the TCP. Bovine HA values were close to zero ($P < 0.0001$; see Fig. 5). BrdU tests show cell proliferation by incorporation of BrdU during DNA synthesis. The results were between 0.6 (TCP), 0.85 (bovine HA) and 0.9 (printed HA; $P < 0.0001$; see Fig. 6).

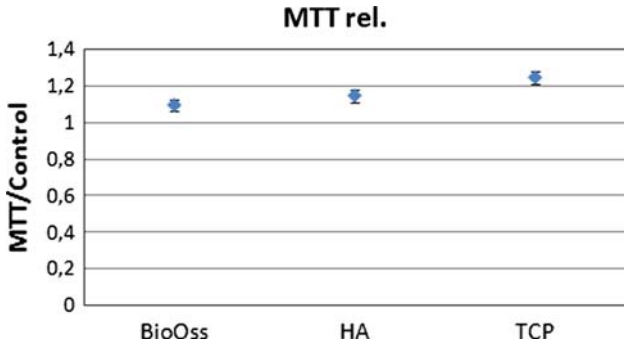

Fig. 4 MTT test of cells from human periosteum on bovine HA, printed HA and printed TCP showing high proliferation rates for all scaffolds tested. Polystyrene served as a control

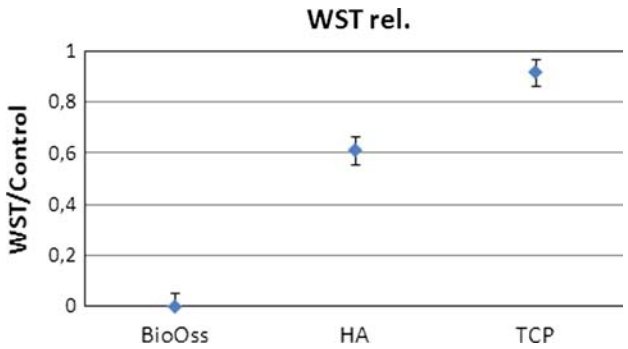

Fig. 5 Successful WST test results of cells from human periosteum on printed HA and printed TCP. Bovine HA showed no proliferation. Polystyrene served as a control

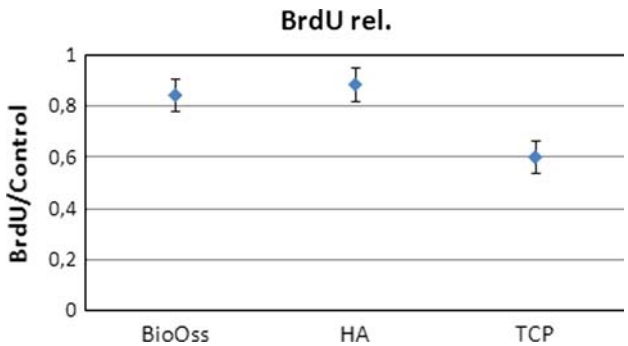

Fig. 6 Proliferation (BrdU) test of cells from human periosteum on bovine HA, printed HA and printed TCP. Polystyrene served as a control

3.3 SEM investigations of cell morphology on membranes

Periosteal cells formed layers covering the surfaces of all scaffolds 7 days after seeding. The representative SEM images in Fig. 7 demonstrate that all scaffolds were covered by cells, which had an elongated morphology with numerous cell pseudopodia, suggesting good biocompatibility.

3.4 Printed scaffolds

The linear sintering shrinkage of the specimen was in the range of 23–25% for the printed TCP and 27–30% for printed HA blocks. The real dimensions of the pore channels were measured to 550 µm for the printed TCP and 480 µm for the printed HA constructs. The microscopic surface texture of the sintered parts was characterized by spherical particles, since the shape of the powder granules was preserved after sintering (see Fig. 7c–f). Consequently, the surface has a big area and a high surface roughness.

4 Discussion

The main goal of augmentations and bone tissue engineering is to create bone. By the use of biomaterials, additional surgical defects for transplant harvesting after tumor surgery or to correct bone hypoplasia or atrophy can be avoided [4]. In this process, biomaterials play a central role [2] as scaffolds for cell attachment, proliferation, and differentiation and to provide the three dimensional structure. On the basis of the results of the SEM investigations, the cell vitality staining and the biocompatibility tests (LDH, MTT, BrdU, WST), it can be concluded from our results that the scaffolds tested are biocompatible for cells derived from human periosteum. This is especially important as augmentation materials have direct contact to the periosteum. The results are in accordance to other investigations: In a study human osteoprogenitor cells derived from periosteum were reimplanted intramuscularly in mice and HA and TCP/HA constructs showed evidence of cell proliferation, calcium deposition, and collagen bundle formation [26].

Hydroxyapatite, the inorganic component of bone [27], is widely used in orthopedic and maxillofacial applications [2, 28]. TCP has also proven to be of good biocompatibility and biodegradability and is extremely osteoconductive [5]. Beta-TCP is known to have the property of complete biodegradation with no adverse biological response. It has the advantage of appropriate porosity to allow osteogenic cell migration, serving as an osteoconductive scaffold for bone ingrowth, retention, and gradual release of osteogenic factors with sufficient strength [29]. In bilateral sinus grafting in patients TCP showed good results [8]. Moreover, combinations of HA and TCP were widely used [9]. After testing the influence of different bone substitute materials on the viability of human osteoblasts it was concluded that HA and TCP support surface- and non-surface-related cell viability [1]. The combination graft of periosteum and beta-TCP showed marked bone formation in rat calvarial defects [16].

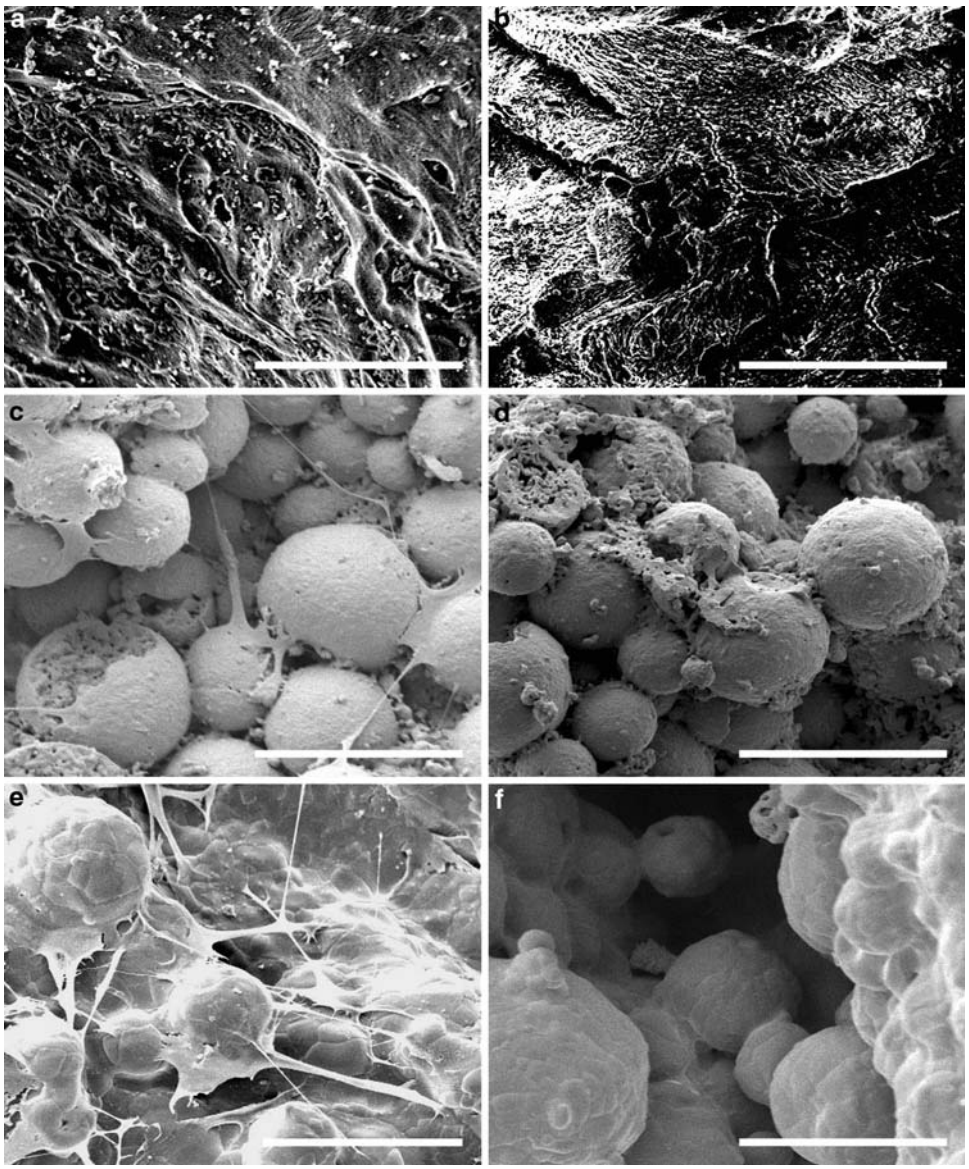

Fig. 7 Close-up SEM images of scaffolds seeded with human periosteal cells and controls 7 days after seeding. The scaffolds were covered by cells with elongated morphology and numerous cell pseudopodia, suggesting good biocompatibility. **a** Bovine HA with cells; **b** bovine HA without cells; **c** printed HA with cells; **d** printed HA without cells; **e** printed TCP with cells; **f** printed TCP without cells. Bar = 50 μm

In earlier stages of endocultivation, it was necessary to use internal scaffolds for bone generation and external scaffolds for stability and form consistency. Bovine hydroxyapatite blocks already displayed successful induction of new bone on the trabeculae [3]. But external titanium meshes are suboptimal because they are non-degradable [30].

The rapid prototyping technique 3D-printing allows for the manufacture of complex-shaped porous ceramic matrices directly from powder materials. Anatomical information obtained from a patient can be used to design the implant for a target defect. As biocompatibility and bone generation of the printed materials is similar to the ones established in our study, future studies may evaluate the stability of larger constructs to generate bone replacements of an individual shape even without external titanium cages. The investigation of differences in osteogenesis and resorption between hydroxyapatite and beta-tricalcium phosphate implanted on the parietal bone of rats revealed that HA blocks were suitable for onlay grafts because of its stability and osteogenesis, while beta-TCP was not stable. [31].

There is growing interest in the use of multipotent mesenchymal stem cells and so-called osteoprogenitor cells harvested from bone marrow or periosteum for in vitro and in vivo osteogenesis. These cells can be differentiated to several cell types by the application of different growth and differentiation factors and suitable matrices as cell adhesives [4, 32–35]. The most important growth factors for differentiation of mesenchymal stem cells to osteogenic cells are BMP-2 and BMP-7 from of the TGF-beta superfamily. Periosteal MSCs are said to be ideal

candidates for utilization in practical bone tissue regeneration [19].

Further in vivo studies should be performed to obtain results in living organisms.

It can be concluded from our data that the 3D-printed hydroxyapatite and 3D-printed TCP as well as bovine HA blocks are biocompatible for cells derived from human periosteum. This is an important issue for augmentations and tissue engineering as periosteal cells have direct contact to the materials in many situations.

Acknowledgements We gratefully acknowledge our laboratory technician Gisela Otto, for her assistance with the analytical and cell culture procedures and Sebastian Spath for his excellent technical assistance. The authors thank the European Union for financial support within the framework of the MyJoint Project (FP-6 NEST 028861).

References

1. Herten M, Rothamel D, Schwarz F, Friesen K, Koegler G, Becker J. Surface- and nonsurface-dependent in vitro effects of bone substitutes on cell viability. Clin Oral Investig. 2009;13:149–55.
2. Turhani D, Weissenbock M, Stein E, Wanschitz F, Ewers R. Exogenous recombinant human BMP-2 has little initial effects on human osteoblastic cells cultured on collagen type I coated/noncoated hydroxyapatite ceramic granules. J Oral Maxillofac Surg. 2007;65:485–93.
3. Warnke PH, Springer IN, Acil Y, Julga G, Wiltfang J, Ludwig K, et al. The mechanical integrity of in vivo engineered heterotopic bone. Biomaterials. 2006;27:1081–7.
4. Warnke PH, Springer IN, Wiltfang J, Acil Y, Eufinger H, Wehmoller M, et al. Growth and transplantation of a custom vascularised bone graft in a man. Lancet. 2004;364:766–70.
5. Arnold U, Lindenhayn K, Perka C. In vitro-cultivation of human periosteum derived cells in bioresorbable polymer-TCP-composites. Biomaterials. 2002;23:2303–10.
6. Cai S, Xu GH, Yu XZ, Zhang WJ, Xiao ZY, Yao KD. Fabrication and biological characteristics of beta-tricalcium phosphate porous ceramic scaffolds reinforced with calcium phosphate glass. J Mater Sci Mater Med. 2009;20:351–8.
7. Gbureck U, Holzel T, Biermann I, Barralet JE, Grover LM. Preparation of tricalcium phosphate/calcium pyrophosphate structures via rapid prototyping. J Mater Sci Mater Med. 2008;19:1559–63.
8. Szabo G, Huys L, Coulthard P, Maiorana C, Garagiola U, Barabas J, et al. A prospective multicenter randomized clinical trial of autogenous bone versus beta-tricalcium phosphate graft alone for bilateral sinus elevation: histologic and histomorphometric evaluation. Int J Oral Maxillofac Implants. 2005;20:371–81.
9. Janssen FW, Oostra J, Oorschot A, van Blitterswijk CA. A perfusion bioreactor system capable of producing clinically relevant volumes of tissue-engineered bone: in vivo bone formation showing proof of concept. Biomaterials. 2006;27:315–23.
10. Alexander D, Hoffmann J, Munz A, Friedrich B, Geis-Gerstorfer J, Reinert S. Analysis of OPLA scaffolds for bone engineering constructs using human jaw periosteal cells. J Mater Sci Mater Med. 2008;19:965–74.
11. Schieker M, Seitz H, Drosse I, Seitz S, Mutschler W. Biomaterials as scaffold for bone tissue engineering. Eur J Trauma. 2006;32:114–24.
12. Li M, Amizuka N, Oda K, Tokunaga K, Ito T, Takeuchi K, et al. Histochemical evidence of the initial chondrogenesis and osteogenesis in the periosteum of a rib fractured model: implications of osteocyte involvement in periosteal chondrogenesis. Microsc Res Tech. 2004;64:330–42.
13. Warnke PH, Douglas T, Sivananthan S, Wiltfang J, Springer I, Becker ST. Tissue engineering of periosteal cell membranes in vitro. Clin Oral Implants Res. 2009;20:761–6.
14. Hutmacher DW. Scaffolds in tissue engineering bone and cartilage. Biomaterials. 2000;21:2529–43.
15. Hutmacher DW, Sittinger M. Periosteal cells in bone tissue engineering. Tissue Eng. 2003;9(Suppl 1):S45–64.
16. Ueno T, Sakata Y, Hirata A, Kagawa T, Kanou M, Shirasu N, et al. The evaluation of bone formation of the whole-tissue periosteum transplantation in combination with beta-tricalcium phosphate (TCP). Ann Plast Surg. 2007;59:707–12.
17. Agata H, Asahina I, Yamazaki Y, Uchida M, Shinohara Y, Honda MJ, et al. Effective bone engineering with periosteum-derived cells. J Dent Res. 2007;86:79–83.
18. Vogelin E, Jones NF, Huang JI, Brekke JH, Lieberman JR. Healing of a critical-sized defect in the rat femur with use of a vascularized periosteal flap, a biodegradable matrix, and bone morphogenetic protein. J Bone Joint Surg Am. 2005;87:1323–31.
19. Hayashi O, Katsube Y, Hirose M, Ohgushi H, Ito H. Comparison of osteogenic ability of rat mesenchymal stem cells from bone marrow, periosteum. and adipose tissue. Calcif Tissue Int. 2008;82:238–47.
20. Zhang X, Awad HA, O'Keefe RJ, Guldberg RE, Schwarz EM. A perspective: engineering periosteum for structural bone graft healing. Clin Orthop Relat Res. 2008;466:1777–87.
21. Breitbart AS, Grande DA, Kessler R, Ryaby JT, Fitzsimmons RJ, Grant RT. Tissue engineered bone repair of calvarial defects using cultured periosteal cells. Plast Reconstr Surg. 1998;101:567–74.
22. Sachs E, Cima M, Williams P, Brancazio D, Cornie J. Three dimensional printing: rapid tooling and prototypes directly from a CAD model. J Eng Ind. 1992;114:481–8.
23. Seitz H, Rieder W, Irsen S, Leukers B, Tille C. Three-dimensional printing of porous ceramic scaffolds for bone tissue engineering. J Biomed Mater Res B Appl Biomater. 2005;74:782–8.
24. Seitz H, Deisinger U, Leukers B, Detsch R, Ziegler G. Different calcium phosphate granules for 3D printing of bone tissue engineering scaffolds. Adv Eng Mater. 2009. Accepted for publication.
25. Yang B, Ludwig K, Adelung R, Kern M. Micro-tensile bond strength of three luting resins to human regional dentin. Dent Mater. 2006;22:45–56.
26. Ng AM, Tan KK, Phang MY, Aziyati O, Tan GH, Isa MR, et al. Differential osteogenic activity of osteoprogenitor cells on HA and TCP/HA scaffold of tissue engineered bone. J Biomed Mater Res A. 2008;85:301–12.
27. Detsch R, Uhl F, Deisinger U, Ziegler G. 3D-cultivation of bone marrow stromal cells on hydroxyapatite scaffolds fabricated by dispense-plotting and negative mould technique. J Mater Sci Mater Med. 2008;19:1491–6.
28. Acil Y, Terheyden H, Dunsche A, Fleiner B, Jepsen S. Three-dimensional cultivation of human osteoblast-like cells on highly porous natural bone mineral. J Biomed Mater Res. 2000;51:703–10.
29. Chen WJ, Jingushi S, Jingushi K, Iwamoto Y. In vivo banking for vascularized autograft bone by intramuscular inoculation of recombinant human bone morphogenetic protein-2 and beta-tricalcium phosphate. J Orthop Sci. 2006;11:283–8.
30. Warnke PH, Wiltfang J, Springer I, Acil Y, Bolte H, Kosmahl M, et al. Man as living bioreactor: fate of an exogenously prepared

customized tissue-engineered mandible. Biomaterials. 2006;27:3163–7.
31. Fujita R, Yokoyama A, Kawasaki T, Kohgo T. Bone augmentation osteogenesis using hydroxyapatite and beta-tricalcium phosphate blocks. J Oral Maxillofac Surg. 2003;61:1045–53.
32. Chang SC, Chuang H, Chen YR, Yang LC, Chen JK, Mardini S, et al. Cranial repair using BMP-2 gene engineered bone marrow stromal cells. J Surg Res. 2004;119:85–91.
33. Iwasaki M, Nakahara H, Nakase T, Kimura T, Takaoka K, Caplan AI, et al. Bone morphogenetic protein 2 stimulates osteogenesis but does not affect chondrogenesis in osteochondrogenic differentiation of periosteum-derived cells. J Bone Miner Res. 1994;9:1195–204.
34. Kubler N, Urist MR. Allogenic bone and cartilage morphogenesis. Rat BMP in vivo and in vitro. J Craniomaxillofac Surg. 1991;19:283–8.
35. Lecanda F, Avioli LV, Cheng SL. Regulation of bone matrix protein expression and induction of differentiation of human osteoblasts and human bone marrow stromal cells by bone morphogenetic protein-2. J Cell Biochem. 1997;67:386–96.